Supporting Information

Cayan et al. 10.1073/pnas.0912391107

SI Text

SI Data and Models.

S1. Observational Data. Daily gridded meteorological observations of precipitation (P), maximum temperature (Tmax), minimum temperature (Tmin), and wind speed at 1/8 degree spatial resolution across the Southwestern Unites States were obtained from the Surface Water Modeling Group at the University of Washington (http://www.hydro.washington.edu; 1). The data are based on the National Weather Service cooperative network of weather observations stations, augmented by information from the higher quality Global Historical Climatology Network (GHCN) stations.

The dataset in ref. 1 is available for the period 1915 through 2003. To extend the dataset up to 2008, we used daily gridded meteorological fields for the period 2004 through 2008 produced by the same group (the Surface Water Modeling Group at the University of Washington) based on a reduced set of stations. This reduced set is available with near-real-time updates, because it is used operationally for a West-wide seasonal hydrologic forecast system (2).

S2. The Variable Infiltration Capacity (VIC) hydrologic model. To produce hydrologic variables during the 20th century and under 21st century climate change conditions, we used the VIC distributed macroscale hydrologic model (3). Defining characteristics of VIC are the probabilistic treatment of subgrid soil moisture capacity distribution, the parameterization of baseflow as a nonlinear recession from the lower soil layer, and the unsaturated hydraulic conductivity at each particular time step is treated as a function of the degree of soil saturation (3, 4). It uses a tiled representation of the land surface within each model grid cell, allowing subgrid variability in topography, infiltration, and land surface vegetation classes (3, 4).

The VIC model was run at a daily time step, with a 1-hour snow model time step in water balance mode, and using a 1/8 by 1/8 degree resolution grid across the Southwestern United States. Using the gridded observed meteorological forcing (described below), along with the physiographic characteristics of the catchment (for example, soil and vegetation), VIC calculates a suite of hydrologic variables, including runoff, baseflow, soil moisture, actual evapotranspiration and snow water equivalent in the snowpack. Derived variables such as radiation, humidity, and pressure are estimated internally based on the input P, Tmax, and Tmin (5, 6).

VIC has been used extensively in a variety of water resources applications; from studies of climate variability, forecasting and climate change studies (2, 4, 7–12). The model's soil moisture estimations produce reasonable agreement with the few point measurements available (4), and VIC-simulated streamflow validates well with observations when the model has been calibrated using streamflow data (4, 12).

VIC was forced using the observed gridded meteorology described above (1, 2), and with downscaled global climate model (GCM) data from 1950 to 2099 using two climate models: the Centre National de Recherches Météorologiques (CNRM) CM3 model, and the Geophysical Fluid Dynamics Laboratory (GFDL) CM2.1 model. We used both the SRES A2 and B1 emissions scenarios in this work. Daily precipitation (P) and maximum and minimum temperatures (Tmax, Tmin) from models were downscaled to 1/8 degree resolution using the constructed analogues (CA) statistical downscaling method (12, 13). For the future simulations, climatological wind speed (computed from the daily wind speed in ref. 4 for the period 1950–1999) was used. The downscaled climate fields are obtained by constructing linear combinations of previously observed weather patterns, including adjustments for model biases and loss of variance. Results using CA and those obtained with bias correction and spatial downscaling (BCSD), another statistical downscaling methodology, are qualitatively similar (13). An advantage of the CA method over the BCSD method is that CA can capture changes in the diurnal cycle of temperatures; the downside is that this requires daily data rather than monthly.

Our soil moisture indices were calculated as follows: (*I*) At each model time step, we combined the instantaneous moistures from VIC's three soil layers. (*ii*) At each point, we computed the maximum soil moisture possible at each point by combining the maximum soil moisture possible in each of the three soil layers. (The maximum soil moisture for each soil layer is equal to soil layer depth multiplied by its respective porosity.) (*iii*) At each model time step, the soil moisture fraction is equal to ratio of instantaneous moisture to the maximum possible moisture. Soil moisture was averaged across Southwest region. In the Southwest, the soil accumulates water from the beginning of the year until April, whereupon it dries until October.

S3. GCM Simulations. For the present study we selected simulations from 12 GCMs from the World Climate Research Program (WCRP) Coupled Model Intercomparison Project phase 3 (CMIP3) multimodel dataset: CNRM CM3, GFDL CM2.1, Center for Climate System Research (University of Tokyo) Model for Interdisciplinary Research On Climate (MIROC) 3.2 (medium resolution), European Center-Hamburg/Max Planck Institute ECHAM5/MPI OM, National Center for Atmospheric Research (NCAR) Community Climate System Model version 3 (CCSM3), NCAR Parallel Climate Model (PCM), Goddard space flight center Coupled General Circulation Model (CGCM) 3.1 (T47), Australian Commonwealth Scientific and Research Organization (CSIRO) Mk 3.0, Institut Pierre Simon Laplace (IPSL) CM4, United Kingdom Meteorological Office (UKMO) HadCM3, and UKMO HadGEM1. Documentation on the models can be found at http://www-pcmdi.llnl.gov/ipcc/model_documentation/pcc_model_documentation.php. These models were selected because they have been evaluated and used in previous investigations of climate change over the region (e.g., 14), so the results herein can be more easily compared to previously published results.

We selected CNRM CM3 and GFDL CM2.1 for detailed analysis because they provided the contiguous daily output of Tmin and Tmax necessary for the VIC hydrological model, and because their simulations lie within the range of temperature and precipitation projections produced by a set of several global climate model simulations of future climate over the Southwest (Fig. S1).

The performance of these two models in terms of their mean climate and variability of temperature and precipitation on seasonal, pentadal, and decadal timescales has been previously evaluated over the western United States (14). Also included in the evaluation was the models' ability to represent El Niño-Southern Oscillation (ENSO), the Pacific Decadal Oscillation (PDO), and the teconnected responses of temperature and precipitation to ENSO and PDO in our region of interest. Over the 42 metrics used, GFDL 2.1 was in the top third of models, whereas CNRM was in the bottom third. CNRM's performance

was hampered by significant biases; however, it is worth pointing out that the downscaling we used removes these biases. In other aspects of its simulation, CNRM was nearer to the middle of the pack of the CMIP3 models.

Both models have an overly strong ENSO signal that extends too far to the west in the tropical Pacific, a common failing of the current generation of global climate models. CNRM also has an ENSO period that is closer to 3 years, while in nature it is more irregular and spreads toward longer timescales. GFDL 2.1 has a good simulation of ENSO's spectrum. Both models have a PDO that is overly trapped to the Kuroshio region off the coast of Japan, rather than having the maximum in the center of the North Pacific. The amplitude of CNRM's PDO is realistic, but GFDL's is too weak along the west coast of North America. GFDL 2.1 again has a spectrum of the PDO that is indistinguishable from observations given the considerable sampling uncertainties involved, while CNRM has an overly pronounced 10-year peak in the spectrum. These model limitations should be kept in mind when evaluating the downscaled results shown here.

We used simulations driven by two greenhouse gas emissions scenarios. The A2 emissions scenario represents a differentiated world in which economic growth is uneven and the income gap remains large between now-industrialized and developing parts of the world; people, ideas, and capital are less mobile so that technology diffuses more slowly. The B1 emissions scenario presents a future with a high level of environmental and social consciousness combined with a globally coherent approach to a more sustainable development. The A2 scenario has higher emissions than the B1 scenario.

S4. Constructing Fig. 5*B*. The observations used to construct Fig. 5*B* in the main text are taken from US Bureau of Reclamation estimates of naturalized flow of the Colorado River at Lees Ferry, updated as of September 16, 2009. Flow values should be considered provisional, especially for the most recent years.

Comparing model-estimated flows to observed flows requires dealing with model biases. Model flows were adjusted to have the same mean and standard deviation as observed over the period 1950–1999. Values for mean and standard deviation are: observations, (14.68,4.64) million acre-feet (maf); for the GFDL model, (17.65,6.18) maf; for CNRM, (16.30,3.99) maf.

Each year in the historical period, 1906–2008, is shown on Fig. 5*B* as a black or red dot. Each year will have an accumulated deficit for every value of the running mean window width N from 1 to 10 (shown on the X axis of the figure). However, the dot is only plotted at the X value that has the maximum accumulated deficit. For example, consider the N-year running mean ending in 1950. Perhaps the 1 year running mean deficit is -2, and the two year running mean deficit is $+3$, and the three year mean deficit is -7, etc., so that all the running mean deficits are $(-2, +3, -7, -5,1,4,0, -2, -1,1)$. In this case a dot would be plotted at $X = 3$, because the three year running mean is the one with the greatest flow deficit. There are different numbers of dots in each vertical column partly by chance, and partly reflecting the typical length of droughts in the region.

1. Hamlet AF, Lettenmaier DP (2005) Production of temporally consistent gridded precipitation and temperature fields for the continental US. *J Hydrometeorol* 6:330–336.
2. Wood AW, Lettenmaier DP (2006) A testbed for new seasonal hydrologic forecasting approaches in the western US. *B Am Meteorol Soc* 87(12):1699–1712.
3. Liang X, Lettenmaier DP, Wood EF, Burges SJ (1994) A simple hydrologically based model of land surface water and energy fluxes for GSMs, *J Geophys Res* 99(D7):14415–14428.
4. Maurer EP, Wood AW, Adam JC, Lettenmaier DP, Nijssen B (2002) A long-term hydrologically based dataset of land surface fluxes and states for the conterminous United States. *J Climate* 15:3237–3251.
5. Kimball JS, Running SW, Nemani R (1997) An improved method for estimating surface humidity from daily minimum temperature. *Agricultural and Forest Meteorol*. 85:87–98.
6. Thornton PE, Running SW (1999) An improved algorithm for estimating incident daily solar radiation from measurements of temperature, humidity, and precipitation. *Agric. For. Meteorol.* 93:211–228.
7. Nijssen B, O'Donnell GM, Lettenmaier DP, Lohmann D, Wood EF (2001) Predicting the discharge of global rivers. *J Climate* 14:3307–3323.
8. Sheffield J, Wood EF (2007) Characteristics of global and regional drought, 1950–2000: Analysis of soil moisture data from off-line simulation of the terrestrial hydrologic cycle. *J Geophys Res* 112(D17115) doi:10.1029/2006JD008288.
9. Barnett TP, et al. (2008) Human-induced changes in the hydrology of the western US. *Science* doi:10.1126/science.1152538.
10. Wood AW, Leung LR, Sridhar V, Lettenmaier DP (2004) Hydrologic implications of dynamical and statistical approaches to downscaling climate model outputs. *Climatic Change* 62:189–216.
11. Das T, et al. (2009) Structure and origins of trends in hydrological measures over the western United States. *J Hydrometeorol* 10:871–892.
12. Hidalgo HG, et al. (2009) Detection and attribution of streamflow timing changes to climate change in the western United States. *J Climate* 22:3838–3855.
13. Maurer EP, Hidalgo HG (2008) Utility of daily vs. monthly large-scale climate data: an intercomparison of two statistical downscaling methods. *Hydrol Earth Syst Sc* 12:551–563.
14. Pierce DW, Barnett TP, Santer BD, Gleckler PJ (2009) Selecting global climate models for regional climate change studies. *Proc Natl Acad Sci* doi:10.1073/pnas.0900094106.

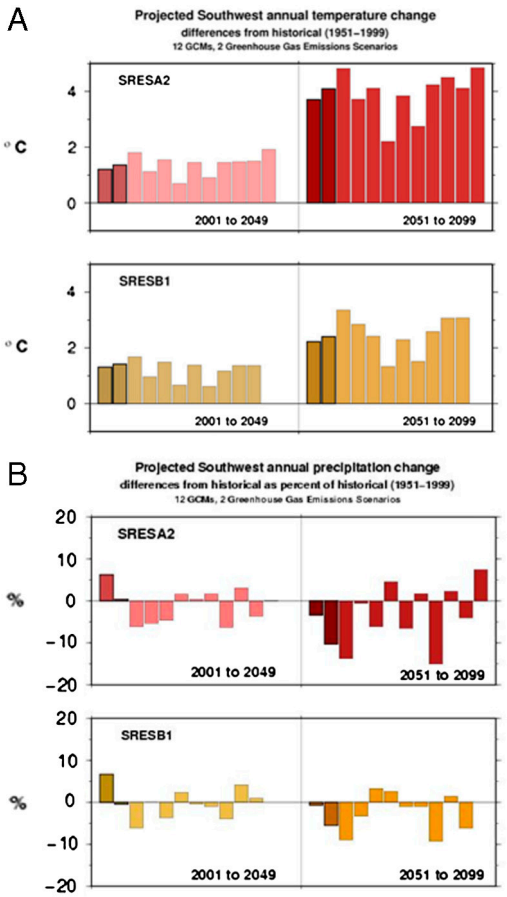

Fig. S1. Projected changes in annual temperature (*A*, *Upper*, °C) and precipitation (*B*, *Lower*, %) from the 12 CGMs used in this study. The 2 models analyzed in further detail (CNRM CM3 and GFDL CM2.1) are shown as outlined bars at the left of each row. Changes are relative to each model's historical period (1951–1999).

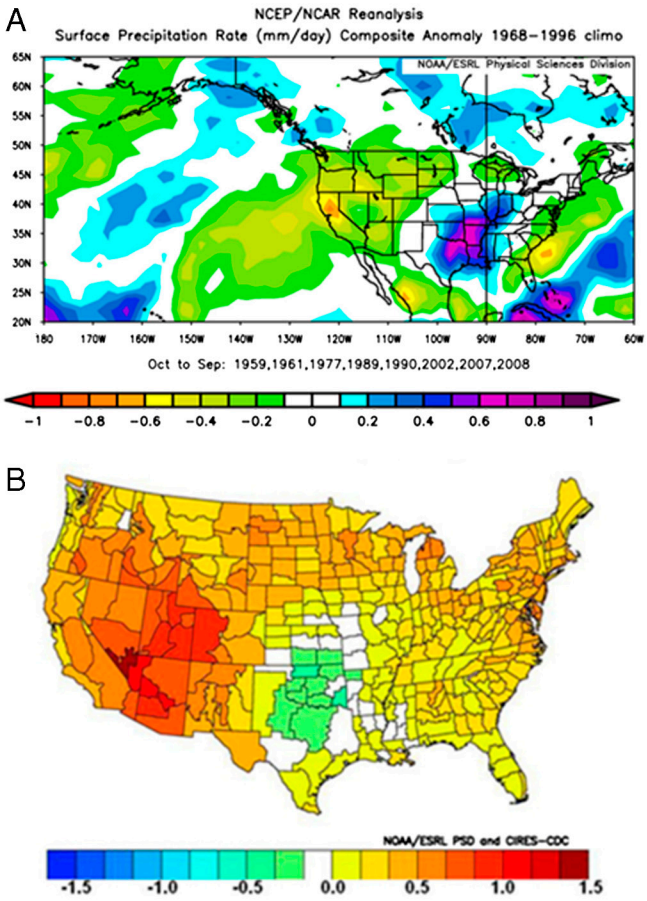

Fig. S2. (*A*, *Upper*) Composite precipitation rate (mm/day) over the water years of the extreme dry soil moisture years from National Center for Environmental Protection/National Center for Atmospheric Research (NCEP/NCAR) Reanalysis. Water years included are 1959, 1961, 1977, 1989, 1990, 2002, 2007, and 2008 (note that the reanalysis data starts in 1950). Water Year defined such that Water Year 2008 is October 2007–September 2008.). (*B*, *Lower*) Composite warm season (April–September) temperature anomalies (°C) during 11 extreme dry soil moisture years. These images are provided by the National Oceanic and Atmospheric Administration/Earth System Research Laboratory (NOAA/ESRL) Physical Sciences Division, Boulder Colorado from their Web site at http://www.psd.noaa.gov/ and use National Climatic Data Center (NCDC), 1994, Time Bias Corrected Divisional Temperature-Precipitation-Drought Index (TD-9640). Documentation for dataset TD-9640 is available from DBMB, NCDC, National Oceanic and Atmostpheric Administration.

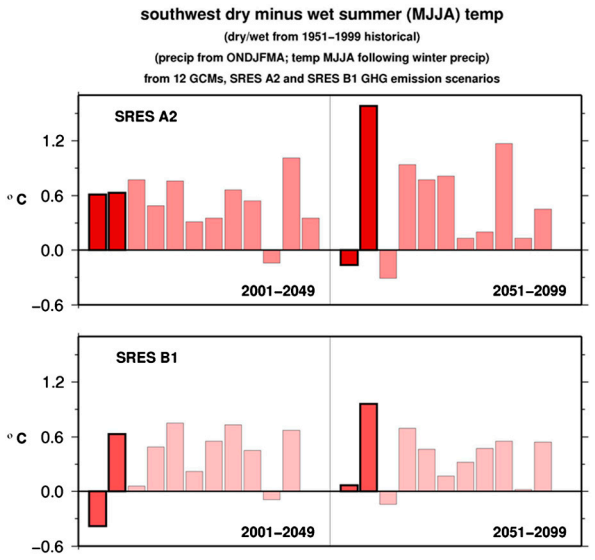

Fig. S3. Difference in May through August mean temperature: During years whose prior October through April precipitation is below average minus temperature for years whose prior October through April precipitation is above average. Scenario IPCC Special Report on Emissions Scenarios (SRES) A2 (*Upper*) and SRES B1 (*Lower*) for 2001–2049 and for 2051–2099.

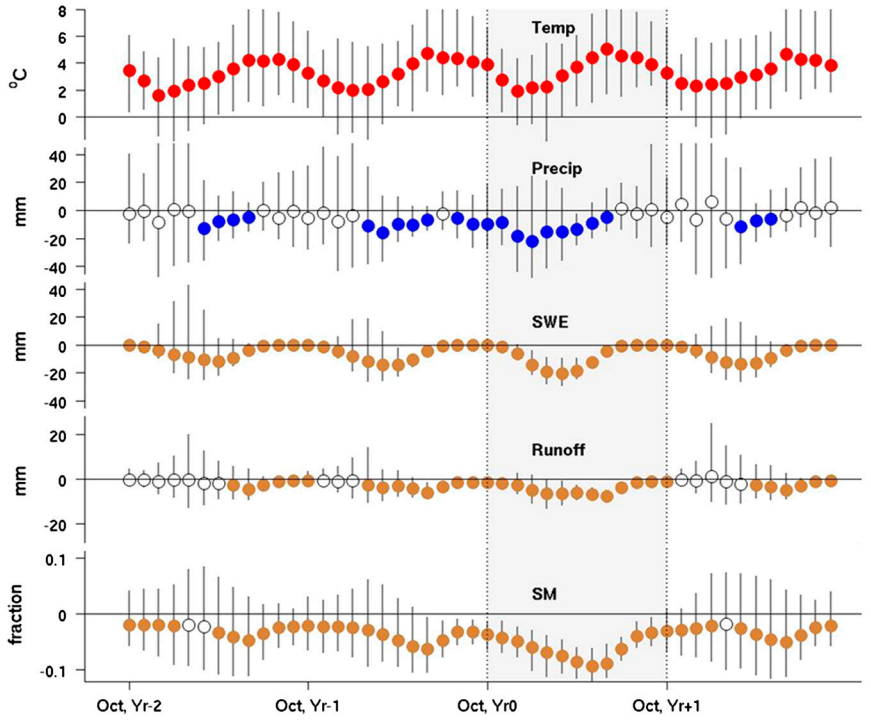

Fig. S4. Composite Southwest-area aggregated monthly anomaly of precipitation, snow water equivalent, runoff, and soil moisture beginning October, two years prior to the extreme drought year through September, one year after the extreme drought year. Composites are average anomalies over the drought cases identified from VIC simulations of CNRM CM3 and GFDL CM2.1 GCMs SRES A2 and SRES B1 emission scenarios, for the late 21st century 2050–2099 period. Composite anomalies (*Circles*) are calculated from 1951–1999 average monthly climatology, and those which are significant at the 95th percentile are colored. Vertical whiskers extend from the 5th percentile to the 95th percentile of the composite samples.

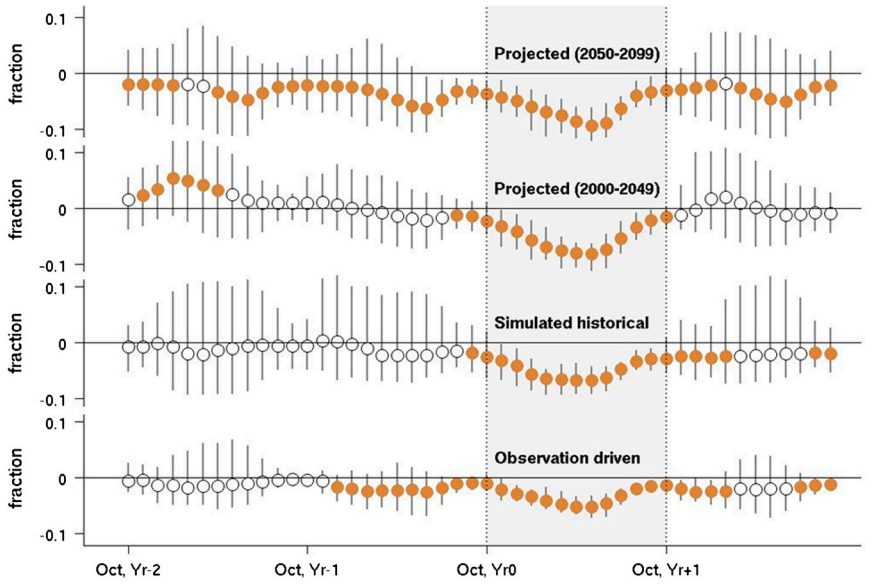

Fig. S5. Soil moisture anomalies composited on dry spells, for the historical period (1951–1999, *Lower Two Panels*), first half of the century, and second half of the century (*Upper Panel*). Values are from VIC driven by observations (*Lower*), and VIC driven by the downscaled CNRM CM3 and GFDL CM2.1 global models (*Other Panels*). Composite anomalies (*Circles*) are calculated from 1951–1999 average monthly climatology, and those which are significant at the 95th percentile are colored. Vertical whiskers extend from the 5th percentile to the 95th percentile of the composite samples.

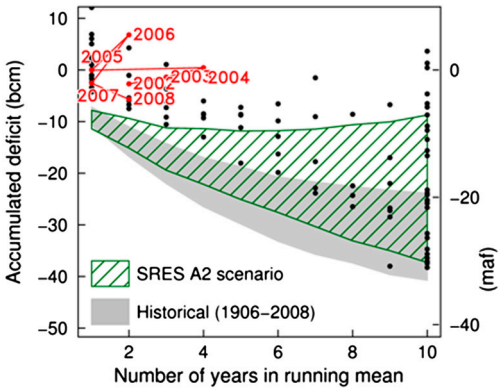

Fig. S6. As Fig. 4*B* in the main text, but calculated for the Sacramento River at Bend Bridge (south of Redding, California).

Table S1. Correlation among annual soil moisture (fraction of saturation) for different regions, in historical and climate change simulations

Correlation of Soil Moisture among Different Regions

1916–1962 (from observed historical VIC simulations)				
	Southwest	*Colorado*	*Great Basin*	*California*
Southwest	1.00	0.76	0.75	0.75
Colorado	0.76	1.00	0.34	0.19
Great Basin	0.75	0.34	1.00	0.59
California	0.75	0.19	0.59	1.00
1963–2008 (from observed historical VIC simulations)				
	Southwest	*Colorado*	*Great Basin*	*California*
Southwest	1.00	0.87	0.94	0.86
Colorado	0.87	1.00	0.74	0.52
Great Basin	0.94	0.74	1.00	0.83
California	0.86	0.52	0.83	1.00
2000–2049 (median of four climate change simulations)				
	Southwest	*Colorado*	*Great Basin*	*California*
Southwest	1.00	0.85	0.90	0.88
Colorado	0.85	1.00	0.61	0.54
Great Basin	0.90	0.61	1.00	0.88
California	0.88	0.54	0.88	1.00
2050–2099 (median of four climate change simulations)				
	Southwest	*Colorado*	*Great Basin*	*California*
Southwest	1.00	0.87	0.92	0.90
Colorado	0.87	1.00	0.67	0.55
Great Basin	0.92	0.67	1.00	0.90
California	0.89	0.55	0.90	1.00

Soil moisture was simulated using VIC as driven by historical observed meteorology and downscaled meteorology from CNRM CM3 and GFDL CM2.1 GCMs, SRES A2 and SRES B1 emissions scenarios. For the climate change period, the median of the four climate change simulations are shown.

Table S2. Historical drought years

Historical Drought Years							
		Southwest				**Great Basin**	
	precip (mm)	*soil moisture (fraction)*	*runoff (mm)*		*precip (mm)*	*soil moisture (fraction)*	*runoff (mm)*
1934	301	0.32	71	*1934*	210	0.38	15
2002	296	0.32	91	*1933*	224	0.38	23
1977	297	0.33	55	*1918*	276	0.39	27
1990	340	0.33	71	*1931*	225	0.39	17
1933	324	0.33	82	*1960*	228	0.39	23
2007	304	0.33	73	*2002*	229	0.39	26
1931	319	0.33	65	*1989*	264	0.40	26
1989	338	0.34	87	*2007*	226	0.40	13
1959	332	0.34	84	*1930*	283	0.40	29
2008	310	0.34	79	*1929*	292	0.40	31
1961	372	0.34	87	*1959*	260	0.40	22
Long Term Mean (1951–1999)	419	0.36	121	*Long Term Mean (1951–1999)*	320	0.43	44
		California				**Colorado**	
	precip (mm)	*soil moisture (fraction)*	*runoff (mm)*		*precip (mm)*	*soil moisture (fraction)*	*runoff (mm)*
1977	334	0.24	128	*2002*	217	0.31	25
1931	388	0.25	155	*1956*	248	0.32	35
1991	428	0.25	170	*1934*	265	0.33	25
1990	418	0.25	176	*1951*	302	0.33	37
1924	321	0.25	146	*1990*	334	0.33	32
2007	392	0.26	197	*1957*	366	0.33	48
1934	437	0.26	191	*1977*	287	0.34	27
2008	425	0.26	210	*1954*	327	0.34	32
1933	452	0.26	207	*1959*	293	0.34	31
1920	429	0.27	177	*1955*	303	0.34	32
1989	493	0.27	222	*1974*	275	0.34	39
Long Term Mean (1951–1999)	596	0.31	301	*Long Term Mean (1951–1999)*	359	0.36	48

A drought year is defined as a water year when the basin or regional aggregate, whole column soil moisture, averaged over the water year, falls below the 1951–1999 10th percentile value. Soil moisture was simulated using VIC as driven by historical observed meteorology. Using this criterion, a separate set of drought years is determined for the Southwest, Great Basin, California, and Colorado regions.